



# Calculation and Forecasting of MTDC Grids' Reliability Indices Considering the Expansion of the Grid and Grid Components' Characteristics

S. P. Ramezanzadeh\*, M. Mirzaie<sup>\*(C.A.)</sup>, M. Shahabi\*

**Abstract:** Due to the role of renewable energy sources in providing energy in future power systems, multi-terminal HVDC (MTDC) systems have attracted the attention of utilities and decision-makers. The reliability study of MTDC grids is critical for analyzing electrical power systems and providing a reliable power delivery system. Reliability modeling and study of six MTDC transmission networks containing hybrid DC circuit breakers for interrupting transmission line contingencies is presented in this paper. This study incorporates precise reliability models of MTDC grid configurations and describes a step-by-step grid expansion. Considering these reliability models, critical reliability indices of the demand bus of the grid have been obtained to calculate the amount of energy not supplied. Also, the influence of the tapping stations on the demand bus reliability features has been investigated. Since the components' characteristics significantly affect the system's reliability, the impact of the transformer and DC circuit breaker's failure rate and repair time on the reliability features of the demand bus of all MTDC grids have been assessed. The obtained results are employed to forecast the effect of simultaneous change of the repair time and failure rate of the transformer, the most influential component in determining the reliability indices, on the proposed configuration by incorporating multivariate linear regression.

**Keywords:** Multi-Terminal HVDC (MTDC), Grid Expansion Study, Transmission Lines, Availability, HVDC Converters, Multivariate Linear Regression.

## 1 Introduction

THE need for a reliable electrical energy source prevails, and utilities plan to achieve highly reliable electricity. Albeit, electricity consumers are experiencing more outages globally. High Voltage Direct Current (HVDC) transmission networks can be helpful for reducing the intensity of such massive interruptions by preventing power system instabilities [1-4].

Iranian Journal of Electrical and Electronic Engineering, 2023. Paper first received 11 Jun 2022, revised 31 Mar 2023, and accepted 15 Apr 2023.

\*The authors are with the faculty of electrical and computer engineering, Babol Noshirvani university of technology, Babol, Iran.

E-mails: [s.ramezanzadeh@modares.ac.ir](mailto:s.ramezanzadeh@modares.ac.ir), [mirzaie@nit.ac.ir](mailto:mirzaie@nit.ac.ir), and [shahabi.m@nit.ac.ir](mailto:shahabi.m@nit.ac.ir).

Corresponding Author: M. Mirzaie.

<https://doi.org/10.22068/IJEEE.19.2.2558>.

Moreover, HVDC transmission networks possess numerous advantages in bulk-power long-distance power transmission, interconnections between different power systems, and submarine transmission cables. Utilities plan to overcome technical challenges in power systems, enhance transmission capacity and system stability, and prevent cascading disturbances. The employment of MTDC transmission networks can assist utilities in this way [5].

In [1], Cost parameters for VSC-HVDC transmission networks have been derived from an extensive set of techno-economic sources. Also, comprehensive economic information has been collected from future and implemented VSC HVDC projects. The proposed methodology, with its merits and demerits, is discussed precisely to clarify the

validity and limitations of the method presented in the study. [2] introduces a new cost parameter collection that provides more accurate investment cost estimates than currently available cost parameter collections. This parameter estimation is based on a review of investment cost parameters, including existing cost parameter sets and information about project costs. By using particle swarm optimization, the overall error function of this methodology is minimized to obtain an optimal parameter set.

In [3], converter and transformer real-time failure models are constructed and evaluated. These models are applied to VSC-based power delivery networks to evaluate crucial reliability features. Also, various sensitivity analyses is carried out to assess the influence of various factors on the system's reliability. In [4], an innovative approach for evaluating the capability of distribution systems to deliver electrical power is introduced. Furthermore, an integrated reliability assessment method is introduced based on Monte Carlo simulation. In [5], a methodology for calculating the reliability and cost of operating MTDC transmission systems is outlined with a comparison that focuses on the benefits of using modular multi-level converters. In [6], the optimal location of distributed energy resources is proposed to improve the reliability and voltage profile of the distribution system. Two distribution networks' feeders affected by a city's outages are taken into account in the simulation. Furthermore, a system adequacy assessment is carried out using Monte Carlo simulation.

In [7], a review of the new progress in reliability assessment of VSC transmission systems is presented. Considering the novel power electronic technologies, the VSC transmission network can be divided into sub-systems, and simulation-based methods can achieve the reliability characteristics of the main components. The reliability analysis methods are investigated, and distinctive modeling approaches are analyzed briefly. In [8], a comprehensive model of a VSC-based MTDC system with a novel optimal power flow model is proposed. An investigation has been performed using the 32-bus Nordic case study. The study results prove that VSC-based MTDC transmission networks can decrease the operation cost. Note that transmission loss reduction of the system is correlated with the VSC-based MTDC grids. In [9], a precise modeling for the reliability of HVDC transmission system is introduced. This model is

processed to be more user-friendly and scalable. Moreover, considering referred procedures, demand bus reliability indices are assessed. The effect of a tapping VSC installment on each index is assessed. In [10], HVDC links were accurately modeled and proposed for multi-zone power systems to improve load frequency monitoring and automatic generation control (AGC). The HVDC link was modeled based on a simple first order transfer function. [11] aims to show the weakness and shortcomings of conventional power systems, such as constrained nature and unsatisfying service qualities. In [12] the most important results of parametric analysis are analyzed using a simplified model of a hybrid switch and proper test systems. The primary objective was to understand the behavior of the new DCB when used as a limiter of the fault current and figure out how switches and system parameters affect the over-current and over-voltage which emerge when the hybrid switch works. In [13], a hybrid reliability model of a VSC installment connected to remote wind farms is proposed based on frequency and duration techniques. In [14], a reliability assessment model and a bi-level unreliability model for a  $\pm 500\text{kV}$  HVDC transmission line are proposed. [15] introduces an accurate reliability representation of a  $\pm 800\text{kV}$  HVDC transmission network. The model aims to present an approach to evaluate the reliability indices of sub-systems of the  $\pm 800\text{kV}$  HVDC transmission project.

Ref. [16] describes a novel method for analyzing reliability in HVDC transmission grids based on a Matrix-Based methodology. The proposed method can calculate the failure probability of HVDC transmission systems by the usage of efficient matrix-based procedures. In [17], it is shown that the frequency and duration approach based on the Markov chain model will reduce the precision of the short-term reliability parameters. Consequently, a short-term integration algorithm is improved to increase the calculation's accuracy. In [18], it is concluded that reliability assessment is commonly an economic analysis seen from a wind farm owner's standpoint for smaller offshore systems. Nevertheless, studying the interaction between offshore and onshore systems in reliability evaluation is crucial for large-scale offshore systems. In [19], a well-structured reliability model for 4 HVDC transmission setups is developed and three reliability features of the demand bus have been studied. In addition, the influence of the load on the demand bus reliability index is examined for each setup.

In this paper, six configurations of MTDC grids are studied. These grids include four four-terminal grids with different numbers of DC links and two four-terminal grids with tap stations in two different grid locations. The grids are illustrated, and different parts of them, including converter stations and DC links, are considered in the reliability assessment. For different parts of the model, the rules for parallel and series components' reliability assessment are employed to form the ultimate reliability model. An appropriate Capacity Outage Probability Table (COPT) is constructed corresponding to each part of the reliability model. Then, the mentioned COPTs are used to provide the reliability model of different MTDC grids (using information given in [19]). Combining the reliability models of mentioned parts will obtain a reliability model of the whole system.

For each grid, failure states with the most probability of occurrence are introduced and based on these failures, five important reliability indices (probability of failure (Q), frequency of failure (F), expected energy not served (EENS), expected duration of load curtailment (EDLC), and expected

load curtailment (ELC)) are evaluated at the load point of the grid by MATLAB. Then, the effect of failure rate and repair time of one VSC station (transformer) component and one transmission line (DC circuit breaker) component is assessed.

### 2 HVDC Grids

Four four-terminal HVDC grids are introduced in this section. The main components of these grids are VSC stations and DC transmission lines. Different configurations of a four-terminal HVDC grid are represented in Fig. 1.

Figure 2 illustrates the layout of a VSC. All the VSC stations of different VSC grids are assumed to be similar.

Cap represents the capacitor; ACF represents AC filters; ACB represents the AC circuit breaker; TRN represents the transformer; VIVs represent converter switches; SRs represent smoothing reactors; DCF represents the DC filter and DCB represents the hybrid DC circuit breaker [19].

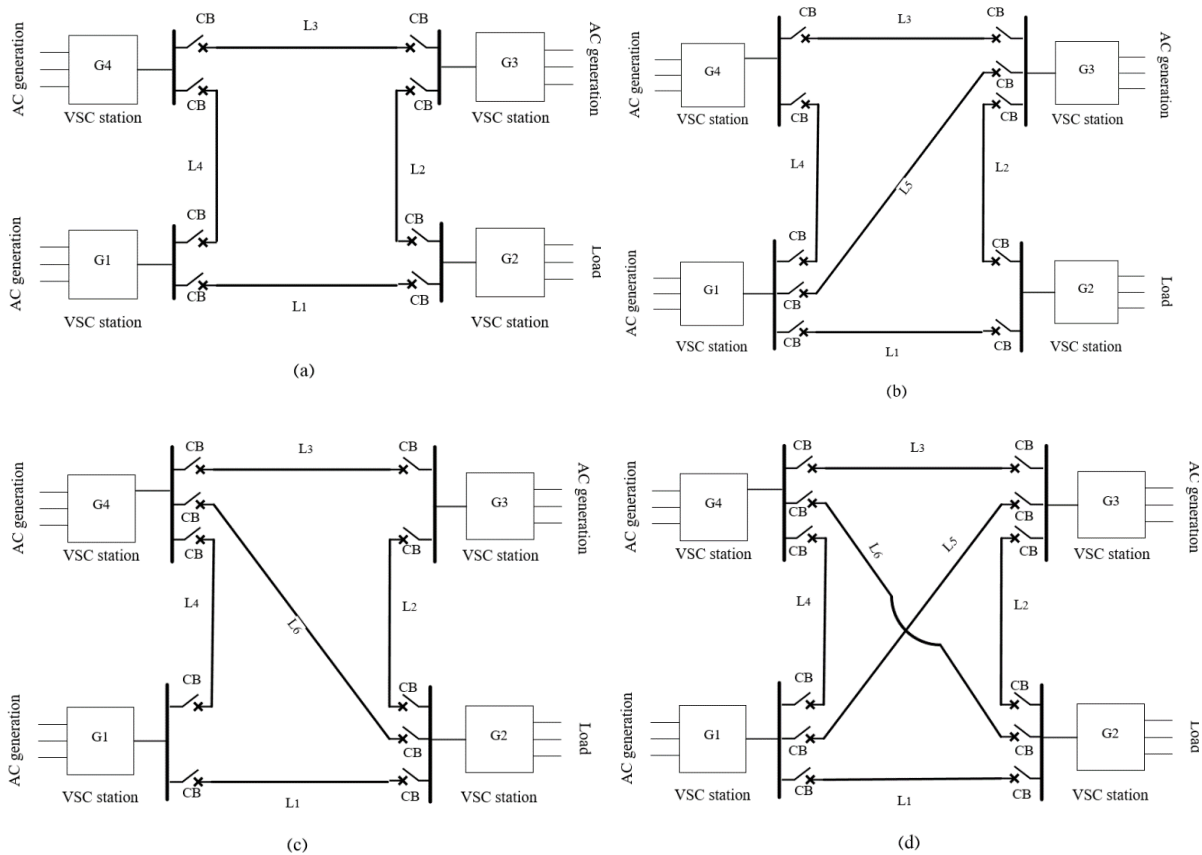


Fig. 1 Four Configurations of four-terminal HVDC grids.

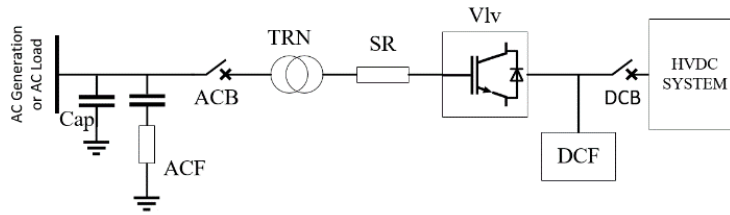


Fig. 2 VSC station [19].

Table 1 HVDC cable characteristics [8-12, 19]

Config. a				
Line	$\lambda$ (occ/yr)	r (hr)	Transmission constraint (MVA)	Length (km)
L1	0.02	1560	-	100
L2	0.02	1560	-	100
L3	0.02	1560	-	100
L4	0.02	1560	-	100
Config. b				
Line	$\lambda$ (occ/yr)	r (hr)	Transmission constraint (MVA)	Length (km)
L1	0.02	1560	-	100
L2	0.02	1560	-	100
L3	0.02	1560	-	100
L4	0.02	1560	-	100
L5	0.03	1560	-	150
Config. c				
Line	$\lambda$ (occ/yr)	r (hr)	Transmission constraint (MVA)	Length (km)
L1	0.02	1560	-	100
L2	0.02	1560	-	100
L3	0.02	1560	-	100
L4	0.02	1560	-	100
L6	0.03	1560	-	150
Config. d				
Line	$\lambda$ (occ/yr)	r (hr)	Transmission constraint (MVA)	Length (km)
L1	0.02	1560	-	100
L2	0.02	1560	-	100
L3	0.02	1560	-	100
L4	0.02	1560	-	100
L5	0.03	1560	-	150
L6	0.03	1560	-	150

Table 2 Maximum injected power in each VSC bus for configurations illustrated in Fig. 1 [19]

Configuration	Maximum generated power in each VSC station (MW)			
	VSC station 1	VSC station 3	VSC station 4	Total generation
Config. a	500	500	400	1400
Config. b	500	500	400	1400
Config. c	500	500	400	1400
Config. d	500	500	400	1400

### 3 Reliability Evaluation and Studied Configurations

DC transmission lines are HVDC cables in this study. There are DC circuit breakers at two ends of the DC cables. Therefore each DCTL has two hybrid breakers and an HVDC cable. HVDC cable characteristics are presented in Table 1. The hybrid circuit breaker is developed in EMTDC/PSCAD software and has shown acceptable performance in fault current interruption.

An MTDC grid with a maximum voltage of 500 kV and hybrid DC circuit breakers is selected for studying the reliability of the MTDC grid's different configurations. The transmission system's AC section is a three-phase electric power installment considered 100% reliable. All the grids illustrated in Fig. 1 have a total generated power of 1400 MW and a total load of 1100 MW. DCTLs, as the link between the VSC bus and the load bus, can maximally transfer 800 MW. On the other hand, their maximum transfer capacity is 600 MW when they connect two VSC station buses. Table 2 shows

the amount of Generated power in each VSC station of the presented HVDC network configurations [19].

The amount of the load is 1100 MW for all configurations. Even though the generated power of VSC stations is not equal, their reliability model is considered to be the same. All the grids (Configs. a-f) have been simulated via PSCAD/EMTDC software to consider the influence of electrical loss. The most electrical loss among different configurations has been generalized to other configurations because the aim was to consider the worst case. As the worst-case electrical loss was almost 50 MW, the total load is considered to be 1150 MW [19].

### 3.1 Reliability Evaluation for Config. a

Different failure states of Config. a are listed in Table 3. The total number of failure states for Config. a is 75, considering a state without failure.

Using the proposed method and information presented in appendices (Tables A1-A3), reliability indices for Config. a will be obtained as they are shown in Table 4. The process of calculating these indices is similar to the method comprehensively described in [19].

**Table 3** Failure states of Config. a.

Failure states	
A converter out	$G_1, G_2, G_3, G_4$
0.35 of a converter out	$0.35G_1, 0.35G_2, 0.35G_3, 0.35G_4$
Two converters out	$G_1G_2, G_1G_3, G_1G_4, G_2G_3, G_2G_4, G_3G_4$
The entire of one and 0.35 of the other converter out	$(0.35G_1)G_2, (0.35G_1)G_3, (0.35G_1)G_4, (0.35G_2)G_1, (0.35G_2)G_3, (0.35G_2)G_4, (0.35G_3)G_1, (0.35G_3)G_2, (0.35G_3)G_4, (0.35G_4)G_1, (0.35G_4)G_2, (0.35G_4)G_3$
0.35 of two converters out	$(0.35G_1)(0.35G_2), (0.35G_1)(0.35G_3), (0.35G_1)(0.35G_4), (0.35G_2)(0.35G_3), (0.35G_2)(0.35G_4), (0.35G_3)(0.35G_4)$
One line out	$L_1, L_2, L_3, L_4$
Two lines out	$L_1L_2, L_1L_3, L_1L_4, L_2L_3, L_2L_4, L_3L_4$
A converter and a line out	$G_1L_1, G_1L_2, G_1L_3, G_1L_4, G_2L_1, G_2L_2, G_2L_3, G_2L_4, G_3L_1, G_3L_2, G_3L_3, G_3L_4, G_4L_1, G_4L_2, G_4L_3, G_4L_4$
0.35 of a converter and a line out	$(0.35G_1)L_1, (0.35G_1)L_2, (0.35G_1)L_3, (0.35G_1)L_4, (0.35G_2)L_1, (0.35G_2)L_2, (0.35G_2)L_3, (0.35G_2)L_4, (0.35G_3)L_1, (0.35G_3)L_2, (0.35G_3)L_3, (0.35G_3)L_4, (0.35G_4)L_1, (0.35G_4)L_2, (0.35G_4)L_3, (0.35G_4)L_4$

**Table 4** Load point indices of Config. a.

Configuration	Q	F(occ/yr)	ELC(MW/yr)	EENS(MWh/yr)	EDLC(hours/yr)
Config. a	0.0481	6.1819	2529.7	175820	421.0587

**Table 5** Failure states of Config. b

Failure states	
A converter out	$G_1, G_2, G_3, G_4$
0.35 of a converter out	$0.35G_1, 0.35G_2, 0.35G_3, 0.35G_4$
Two converters out	$G_1G_2, G_1G_3, G_1G_4, G_2G_3, G_2G_4, G_3G_4$
The entire of one and 0.35 of the other converter out	$(0.35G_1)G_2, (0.35G_1)G_3, (0.35G_1)G_4, (0.35G_2)G_1, (0.35G_2)G_3, (0.35G_2)G_4, (0.35G_3)G_1, (0.35G_3)G_2, (0.35G_3)G_4, (0.35G_4)G_1, (0.35G_4)G_2, (0.35G_4)G_3$
0.35 of two converters out	$(0.35G_1)(0.35G_2), (0.35G_1)(0.35G_3), (0.35G_1)(0.35G_4), (0.35G_2)(0.35G_3), (0.35G_2)(0.35G_4), (0.35G_3)(0.35G_4)$
One line out	$L_1, L_2, L_3, L_4, L_5$
Two lines out	$L_1L_2, L_1L_3, L_1L_4, L_1L_5, L_2L_3, L_2L_4, L_2L_5, L_3L_4, L_3L_5, L_4L_5$
A converter and a line out	$G_1L_1, G_1L_2, G_1L_3, G_1L_4, G_1L_5, G_2L_1, G_2L_2, G_2L_3, G_2L_4, G_2L_5, G_3L_1, G_3L_2, G_3L_3, G_3L_4, G_3L_5, G_4L_1, G_4L_2, G_4L_3, G_4L_4, G_4L_5$
0.35 of a converter and a line out	$(0.35G_1)L_1, (0.35G_1)L_2, (0.35G_1)L_3, (0.35G_1)L_4, (0.35G_1)L_5, (0.35G_2)L_1, (0.35G_2)L_2, (0.35G_2)L_3, (0.35G_2)L_4, (0.35G_2)L_5, (0.35G_3)L_1, (0.35G_3)L_2, (0.35G_3)L_3, (0.35G_3)L_4, (0.35G_3)L_5, (0.35G_4)L_1, (0.35G_4)L_2, (0.35G_4)L_3, (0.35G_4)L_4, (0.35G_4)L_5$

**Table 6** Load point indices of Config. b.

Configuration	Q	F(occ/yr)	ELC(MW/yr)	EENS(MWh/yr)	EDLC(hours/yr)
Config. b	0.0480	6.3656	2591	174970	420.79

**Table 7** Failure states of Config. c.

Failure states	
A converter out	$G_1, G_2, G_3, G_4$
0.35 of a converter out	$0.35G_1, 0.35G_2, 0.35G_3, 0.35G_4$
Two converters out	$G_1G_2, G_1G_3, G_1G_4, G_2G_3, G_2G_4, G_3G_4$
The entire of one and 0.35 of the other converter out	$(0.35G_1)G_2, (0.35G_1)G_3, (0.35G_1)G_4, (0.35G_2)G_1, (0.35G_2)G_3, (0.35G_2)G_4, (0.35G_3)G_1, (0.35G_3)G_2, (0.35G_3)G_4, (0.35G_4)G_1, (0.35G_4)G_2, (0.35G_4)G_3$
0.35 of two converters out	$(0.35G_1)(0.35G_2), (0.35G_1)(0.35G_3), (0.35G_1)(0.35G_4), (0.35G_2)(0.35G_3), (0.35G_2)(0.35G_4), (0.35G_3)(0.35G_4)$
One line out	$L_1, L_2, L_3, L_4, L_6$
Two lines out	$L_1L_2, L_1L_3, L_1L_4, L_1L_6, L_2L_3, L_2L_4, L_2L_6, L_3L_4, L_3L_6, L_4L_6$
A converter and a line out	$G_1L_1, G_1L_2, G_1L_3, G_1L_4, G_1L_6, G_2L_1, G_2L_2, G_2L_3, G_2L_4, G_2L_6, G_3L_1, G_3L_2, G_3L_3, G_3L_4, G_3L_6, G_4L_1, G_4L_2, G_4L_3, G_4L_4, G_4L_6$
0.35 of a converter and a line out	$(0.35G_1)L_1, (0.35G_1)L_2, (0.35G_1)L_3, (0.35G_1)L_4, (0.35G_1)L_6, (0.35G_2)L_1, (0.35G_2)L_2, (0.35G_2)L_3, (0.35G_2)L_4, (0.35G_2)L_6, (0.35G_3)L_1, (0.35G_3)L_2, (0.35G_3)L_3, (0.35G_3)L_4, (0.35G_3)L_6, (0.35G_4)L_1, (0.35G_4)L_2, (0.35G_4)L_3, (0.35G_4)L_4, (0.35G_4)L_6$

**Table 8** Load point indices of Config. c.

Configuration	Q	F(occ/yr)	ELC(MW/yr)	EENS(MWh/yr)	EDLC(hours/yr)
Config. c	0.0311	5.1746	2146	121660	272.1843

### 3.2 Reliability Evaluation for Config. b

Different failure states of Config. b are listed in Table 5. The total number of failure states for Config. b is 88 states.

Using the proposed method and information presented in [19], reliability indices for Config. b will be calculated. The calculated indices are shown in Table 6.

### 3.3 Reliability Evaluation for Config. c

Different failure states of Config. c are listed in Table 7. The total number of failure states for Config. c is 88 states.

Using the proposed method and information presented in appendices, reliability indices for Config. c will be calculated. The calculated indices are shown in Table 8.

As it is obvious, in Config. b, a DC link ( $L_5$ ) is added between VSC stations 1 and 3. A minor improvement in the reliability indices is observable by adding this link. For example, the EENS has decreased by about 0.48 % by adding  $L_5$ . On the other hand, by adding  $L_6$  between VSC stations 2 and 4 (which has been illustrated in Config. c), a

significant improvement in the reliability indices has occurred. For example, the EENS has decreased by about 31 % by adding  $L_6$ .

### 3.4 Reliability Evaluation for Config. d

Different failure states of Config. d are listed in Table 9. The total number of failure states for Config. d is 102 states.

Using the proposed method and information presented in appendices, reliability indices for Config. d will be calculated. The calculated indices have been shown in Table 10.

## 4 The Effect of Tapping Station on the Reliability of Load Point

A four-terminal network, including a tapping station with 300 MW of electrical power, has been introduced in Fig. 3 as Config. e. The total consumption of electrical power (the load and the electrical loss) is considered to be 1150 MW. The VSC tapping station has similar reliability characteristics to other VSC stations, and it is located precisely between terminal 2 and terminal 3, which makes the length of both  $L_2$  and  $L_3$  about 50 km.

**Table 9** Failure states of Config. d.

Failure states	
A converter out	$G_1, G_2, G_3, G_4$
0.35 of a converter out	$0.35G_1, 0.35G_2, 0.35G_3, 0.35G_4$
Two converters out	$G_1G_2, G_1G_3, G_1G_4, G_2G_3, G_2G_4, G_3G_4$
The entire of one and 0.35 of the other converter out	$(0.35G_1)G_2, (0.35G_1)G_3, (0.35G_1)G_4, (0.35G_2)G_1, (0.35G_2)G_3, (0.35G_2)G_4, (0.35G_3)G_1, (0.35G_3)G_2, (0.35G_3)G_4, (0.35G_4)G_1, (0.35G_4)G_2, (0.35G_4)G_3$
0.35 of two converters out	$(0.35G_1)(0.35G_2), (0.35G_1)(0.35G_3), (0.35G_1)(0.35G_4), (0.35G_2)(0.35G_3), (0.35G_2)(0.35G_4), (0.35G_3)(0.35G_4)$
One line out	$L_1, L_2, L_3, L_4, L_5, L_6$
Two lines out	$L_1L_2, L_1L_3, L_1L_4, L_1L_5, L_1L_6, L_2L_3, L_2L_4, L_2L_5, L_2L_6, L_3L_4, L_3L_5, L_3L_6, L_4L_5, L_4L_6, L_5L_6$
A converter and a line out	$G_1L_1, G_1L_2, G_1L_3, G_1L_4, G_1L_5, G_1L_6, G_2L_1, G_2L_2, G_2L_3, G_2L_4, G_2L_5, G_2L_6, G_3L_1, G_3L_2, G_3L_3, G_3L_4, G_3L_5, G_3L_6, G_4L_1, G_4L_2, G_4L_3, G_4L_4, G_4L_5, G_4L_6$
0.35 of a converter and a line out	$(0.35G_1)L_1, (0.35G_1)L_2, (0.35G_1)L_3, (0.35G_1)L_4, (0.35G_1)L_5, (0.35G_1)L_6, (0.35G_2)L_1, (0.35G_2)L_2, (0.35G_2)L_3, (0.35G_2)L_4, (0.35G_2)L_5, (0.35G_2)L_6, (0.35G_3)L_1, (0.35G_3)L_2, (0.35G_3)L_3, (0.35G_3)L_4, (0.35G_3)L_5, (0.35G_3)L_6, (0.35G_4)L_1, (0.35G_4)L_2, (0.35G_4)L_3, (0.35G_4)L_4, (0.35G_4)L_5, (0.35G_4)L_6$

**Table 10** Load point indices of Config. d.

Configuration	Q	F(occ/yr)	ELC(MW/yr)	EENS(MWh/yr)	EDLC(hours/yr)
Config. d	0.0307	5.1623	2151.4	121530	270.8593

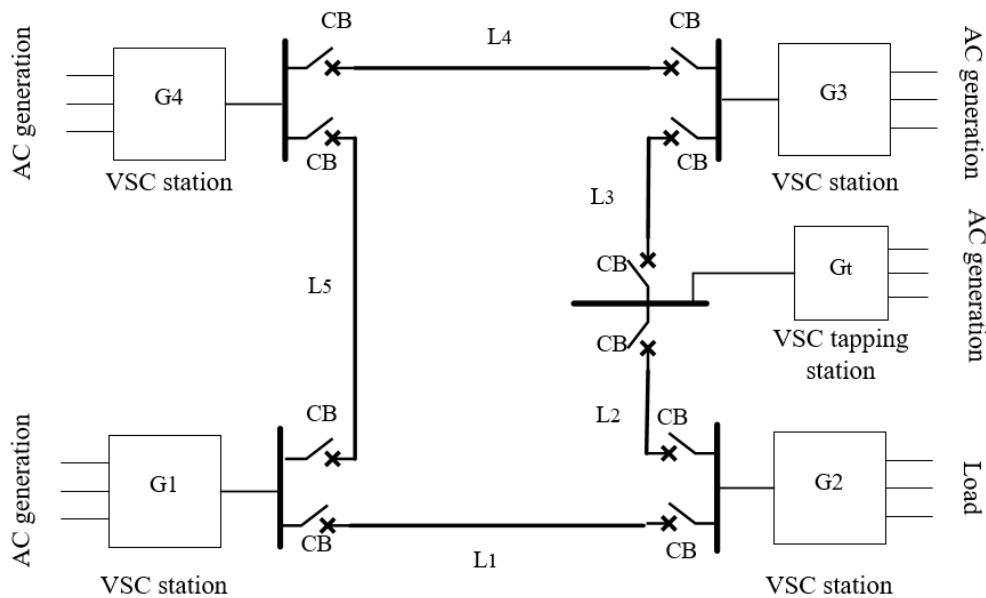


**Fig. 3** A network with a tapping station (Config. e).

Since the grid structure is symmetrical, installing a tapping station between terminal 1 and terminal 2 is similar to incorporating a tapping station between terminal 2 and terminal 3 and gives the same amount of load point reliability indices. Failure states of Config. e have been shown in Table 11. The total number of failure states for Config. e is 116 states.

Using the proposed method and information presented in appendices, reliability indices for

Config. e will be calculated. The calculated indices are shown in Table 12.

A network with a different location of the tapping station has been introduced in Fig.4 as Config. f. The VSC tapping station has similar reliability characteristics to other VSC stations, and it is located precisely between terminal 1 and terminal 4, which makes the length of both  $L_4$  and  $L_5$  about 50 km.

**Table 11** Failure states of Config. e.

Failure states	
A converter out	$G_1, G_2, G_3, G_4, G_t$
0.35 of a converter out	$0.35G_1, 0.35G_2, 0.35G_3, 0.35G_4, 0.35 G_t$
Two converters out	$G_1G_2, G_1G_3, G_1G_4, G_1G_t, G_2G_3, G_2G_4, G_2G_t, G_3G_4, G_3G_t, G_4G_t$
The entire of one and 0.35 of the other converter out	$(0.35G_1)G_2, (0.35G_1)G_3, (0.35G_1)G_4, (0.35G_1)G_t, (0.35G_2)G_1, (0.35G_2)G_3, (0.35G_2)G_4, (0.35G_2)G_t, (0.35G_3)G_1, (0.35G_3)G_2, (0.35G_3)G_4, (0.35G_3)G_t, (0.35G_4)G_1, (0.35G_4)G_2, (0.35G_4)G_3, (0.35G_4)G_t, (0.35G_t)G_1, (0.35G_t)G_2, (0.35G_t)G_3, (0.35G_t)G_4, (0.35G_t)G_5$
0.35 of two converters out	$(0.35G_1)(0.35G_2), (0.35G_1)(0.35G_3), (0.35G_1)(0.35G_4), (0.35G_1)(0.35G_t), (0.35G_2)(0.35G_3), (0.35G_2)(0.35G_4), (0.35G_2)(0.35G_t), (0.35G_3)(0.35G_4), (0.35G_3)(0.35G_t), (0.35G_4)(0.35G_t)$
One line out	$L_1, L_2, L_3, L_4, L_5$
Two lines out	$L_1L_2, L_1L_3, L_1L_4, L_1L_5, L_2L_3, L_2L_4, L_2L_5, L_3L_4, L_3L_5, L_4L_5$
A converter and a line out	$G_1L_1, G_1L_2, G_1L_3, G_1L_4, G_1L_5, G_2L_1, G_2L_2, G_2L_3, G_2L_4, G_2L_5, G_3L_1, G_3L_2, G_3L_3, G_3L_4, G_3L_5, G_4L_1, G_4L_2, G_4L_3, G_4L_4, G_4L_5, G_tL_1, G_tL_2, G_tL_3, G_tL_4, G_tL_5$
0.35 of a converter and a line out	$(0.35G_1)L_1, (0.35G_1)L_2, (0.35G_1)L_3, (0.35G_1)L_4, (0.35G_1)L_5, (0.35G_2)L_1, (0.35G_2)L_2, (0.35G_2)L_3, (0.35G_2)L_4, (0.35G_2)L_5, (0.35G_3)L_1, (0.35G_3)L_2, (0.35G_3)L_3, (0.35G_3)L_4, (0.35G_3)L_5, (0.35G_4)L_1, (0.35G_4)L_2, (0.35G_4)L_3, (0.35G_4)L_4, (0.35G_4)L_5, (0.35G_t)L_1, (0.35G_t)L_2, (0.35G_t)L_3, (0.35G_t)L_4, (0.35G_t)L_5$

**Table 12** Load point indices of Config. e.

Configuration	Q	F(occ/yr)	ELC(MW/yr)	EENS(MWh/yr)	EDLC(hours/yr)
Config. e	0.0329	4.3095	1921.3	131710	280.1

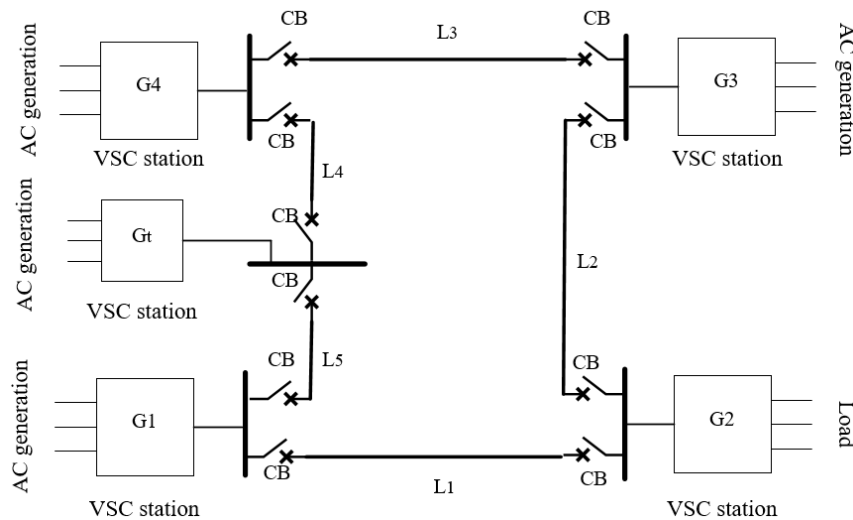


**Fig. 4** A network with a tapping station (Config. f).

Failure states of Config. f have been shown in Table 13. The total number of failure states for Config. f is 116 states.

Incorporating a tapping station between terminal 3 and terminal 4 is similar to incorporating a tapping station between terminal 1 and terminal 4 and gives the same amount of load point reliability indices. Using the proposed method and information presented in appendices, reliability indices for Config. f will be calculated. The calculated indices are shown in Table 14.

In Table 15, the reliability indices of the load point for Config. a-f are presented, and the ratio of Q, F, ELC, EENS, and EDLC of Config. b-f to these

indices of Config. a is calculated. Therefore, any improvement in reliability indices of the load point caused by adding extra DC links or tapping stations will be observable. Based on the obtained results, Config. f has the most negligible probability of failure (0.0193), and Config. a has the most probability of failure (0.0481). Although Config. f has a lesser probability of failure than Config. e, but Config. e has a lesser amount of EENS, which makes the location of the tapping station a critical factor in improving the reliability indices of a grid. In Config. b, there is a link between station 1 and station 3, and the existence of this link improves the reliability indices slightly.



**Table 13** Failure states of Config. f.

Failure states	
A converter out	$G_1, G_2, G_3, G_4, G_t$
0.35 of a converter out	$0.35G_1, 0.35G_2, 0.35G_3, 0.35G_4, 0.35 G_t$
Two converters out	$G_1G_2, G_1G_3, G_1G_4, G_1G_t, G_2G_3, G_2G_4, G_2G_t, G_3G_4, G_3G_t, G_4G_t$
The entire of one and 0.35 of the other converter out	$(0.35G_1)G_2, (0.35G_1)G_3, (0.35G_1)G_4, (0.35G_1)G_t, (0.35G_2)G_1, (0.35G_2)G_3, (0.35G_2)G_4, (0.35G_2)G_t, (0.35G_3)G_1, (0.35G_3)G_2, (0.35G_3)G_4, (0.35G_3)G_t, (0.35G_4)G_1, (0.35G_4)G_2, (0.35G_4)G_3, (0.35G_4)G_t, (0.35G_t)G_1, (0.35G_t)G_2, (0.35G_t)G_3, (0.35G_t)G_4, (0.35G_t)G_5$
0.35 of two converters out	$(0.35G_1)(0.35G_2), (0.35G_1)(0.35G_3), (0.35G_1)(0.35G_4), (0.35G_1)(0.35G_t), (0.35G_2)(0.35G_3), (0.35G_2)(0.35G_4), (0.35G_2)(0.35G_t), (0.35G_3)(0.35G_4), (0.35G_3)(0.35G_t), (0.35G_4)(0.35G_t)$
One line out	$L_1, L_2, L_3, L_4, L_5$
Two lines out	$L_1L_2, L_1L_3, L_1L_4, L_1L_5, L_2L_3, L_2L_4, L_2L_5, L_3L_4, L_3L_5, L_4L_5$
A converter and a line out	$G_1L_1, G_1L_2, G_1L_3, G_1L_4, G_1L_5, G_2L_1, G_2L_2, G_2L_3, G_2L_4, G_2L_5, G_3L_1, G_3L_2, G_3L_3, G_3L_4, G_3L_5, G_4L_1, G_4L_2, G_4L_3, G_4L_4, G_4L_5, G_tL_1, G_tL_2, G_tL_3, G_tL_4, G_tL_5$
0.35 of a converter and a line out	$(0.35G_1)L_1, (0.35G_1)L_2, (0.35G_1)L_3, (0.35G_1)L_4, (0.35G_1)L_5, (0.35G_2)L_1, (0.35G_2)L_2, (0.35G_2)L_3, (0.35G_2)L_4, (0.35G_2)L_5, (0.35G_3)L_1, (0.35G_3)L_2, (0.35G_3)L_3, (0.35G_3)L_4, (0.35G_3)L_5, (0.35G_4)L_1, (0.35G_4)L_2, (0.35G_4)L_3, (0.35G_4)L_4, (0.35G_4)L_5, (0.35G_t)L_1, (0.35G_t)L_2, (0.35G_t)L_3, (0.35G_t)L_4, (0.35G_t)L_5$

**Table 14** Load point indices of Config. f.

Configuration	Q	F(occ/yr)	ELC(MW/yr)	EENS(MWh/yr)	EDLC(hours/yr)
Config. f	0.0193	3.74	1895.5	133550	234.2642

**Table 15** The reliability indices of the load point for Configs. a-f.

Configuration	Q	Q/ Q <sub>config. a</sub>	F(occ/yr)	F/ F <sub>config. a</sub>	ELC (MW/yr)	ELC/ ELC <sub>config. a</sub>	EENS (MWh/yr)	EENS/ EENS <sub>config. a</sub>	EDLC (hours/yr)	EDLC/ EDLC <sub>config. a</sub>
Config. a	0.0482	1.000	6.182	1.000	2529.7	1.000	175820	1.000	421.059	1.000
Config. b	0.0481	0.998	6.366	1.030	2591.0	1.024	174970	0.995	420.790	0.999
Config. c	0.0314	0.646	5.175	0.837	2146.0	0.848	121660	0.692	272.184	0.646
Config. d	0.0309	0.640	5.162	0.835	2151.4	0.850	121530	0.691	270.859	0.643
Config. e	0.0331	0.684	4.309	0.697	1921.3	0.760	131710	0.749	280.100	0.665
Config. f	0.0197	0.400	3.740	0.605	1895.5	0.750	133550	0.760	234.264	0.556

But in Config. c, the existence of a link between station 2 and station 4 improves the reliability indices dramatically. In Config. d, which has both links mentioned above, the reliability indices have been improved slightly compared to Config. c. Concerning the results, the DC link between station 1 and station 3 has a minor impact on the improvement of the reliability indices, while the DC link between station 2 and station 4 significantly influences the improvement of the reliability indices.

### 5 The Effect of the Failure Rate of TRN and DCB on the Reliability of Load Point

TRN and DCB are two components that considerably impact the reliability of the load point. Therefore, the impact of the change of the TRN and DCB failure rate on the reliability indices is investigated in this section and shown in Tables 16 and 17, respectively. For each grid, the components'

failure rate is changed between 0.5 p.u and 2 p.u of the nominal failure rate mentioned in [19], and the reliability indices have been evaluated. Then, the amount of these indices has been divided by the nominal amount of these indices shown in Tables 4, 6, 8, 10, 12, and 14. Therefore, the per-unit amount of each index is obtained and is suitable for comparison with the primary situation.

The most increase of EENS between 0.5 p.u and 2 p.u of the failure rate of TRN is related to Config. d, which increases by 0.2767 p.u. The least increase of EENS between the failure rates of 0.5 p.u and 2 p.u is related to Config. f, which increases by 0.1639 p.u.

The most increase of EENS between 0.5 p.u and 2 p.u of the failure rate of DCB is related to Config. d, which increases by 0.5336 p.u. The least increase of EENS between the failure rates of 0.5 p.u and 2 p.u is related to Config. f, which increases by 0.3168 p.u.

**Table 16** The effect of changing TRN's failure rate on Config. a-f reliability indices.

Config. a						Config. b					
Failure rate in p.u.	Q (p.u.)	F (p.u.)	ELC (p.u.)	EENS (p.u.)	EDLC (p.u.)	Failure rate in p.u.	Q (p.u.)	F (p.u.)	ELC (p.u.)	EENS (p.u.)	EDLC (p.u.)
0.5	0.941788	0.990974	0.987469	0.936583	0.943099	0.5	0.94374	0.990794	0.987264	0.936561	0.947860
0.8	0.977131	0.996457	0.99498	0.974633	0.977275	0.8	0.97708	0.995978	0.994983	0.974624	0.977257
1.1	1.010395	1.001796	1.00249	1.012683	1.011355	1.1	1.01250		1.002702	1.012688	1.011360
1.4	1.043659	1.007215	1.010001	1.05062	1.045365	1.4	1.04583		1.010035	0.010505	1.045391
1.7	1.079002	1.012634	1.017512	1.088556	1.079303	1.7	1.07916	1.013259	1.017754	1.088701	1.079325
2.0	1.112266	1.017972	1.025023	1.126436	1.113166	2.0	1.11458	1.018443	1.025473	1.126650	1.113188

Config. c						Config. d					
Failure rate in p.u.	Q (p.u.)	F (p.u.)	ELC (p.u.)	EENS (p.u.)	EDLC (p.u.)	Failure rate in p.u.	Q (p.u.)	F (p.u.)	ELC (p.u.)	EENS (p.u.)	EDLC (p.u.)
0.5	0.909968	0.988096	0.984157	0.907776	0.910449	0.5	0.912052	0.987544	0.984010	0.907595	0.909697
0.8		0.995246	0.993476	0.963094	0.964222	0.8	0.964169	0.995022	0.993539	0.963054	0.963932
1.1	1.016077	1.002396	1.003262	1.018412	0.834177	1.1	1.019544	1.002499	1.003068	1.018432	1.018019
1.4		1.009547	1.012582	1.073648	1.071395	1.4	1.074919	1.009957	1.012829	1.073809	1.071988
1.7	1.122186	1.016697	1.021901	1.128802	1.124789	1.7	1.127036	1.016989	1.022590	1.129104	1.125824
2.0	1.176849	1.024234	1.031221	1.183955	1.178090	2.0	1.182410	1.024737	1.032351	1.184317	1.179542

Config. e						Config. f					
Failure rate in p.u.	Q (p.u.)	F (p.u.)	ELC (p.u.)	EENS (p.u.)	EDLC (p.u.)	Failure rate in p.u.	Q (p.u.)	F (p.u.)	ELC (p.u.)	EENS (p.u.)	EDLC (p.u.)
0.5	0.969605	0.992250	0.985791	0.944575	0.976151	0.5	0.948187	0.991979	0.985492	0.945414	0.970998
0.8	0.987842	0.996891	0.994119	0.977830	0.990432	0.8	0.979275	0.997620	0.994461	0.978136	0.988393
1.1	1.003040	1.001555	1.002967	1.011085	1.004784	1.1	1.010363	1.003182	1.002902	1.010932	1.005813
1.4	1.021277	1.006219	1.011294	1.044340	1.019151	1.4	1.041451	1.008717	1.011343	1.043729	1.023289
1.7	1.039514	1.010860	1.020143	1.077595	1.033559	1.7	1.072539	1.014251	1.020311	1.076526	1.040791
2.0	1.057751	1.015524	1.028470	1.110850	1.047840	2.0	1.103627	1.019813	1.028752	1.109322	1.058378

**Table 17** The effect of changing the failure rate of DCB on reliability indices of Configs. a-f.

Config. a						Config. b					
Failure rate in p.u.	Q (p.u.)	F (p.u.)	ELC (p.u.)	EENS (p.u.)	EDLC (p.u.)	Failure rate in p.u.	Q (p.u.)	F (p.u.)	ELC (p.u.)	EENS (p.u.)	EDLC (p.u.)
0.5	0.941788	0.990974	0.987469	0.936583	0.943099	0.5	0.94374	0.990794	0.987264	0.936561	0.947860
0.8	0.977131	0.996457	0.99498	0.974633	0.977275	0.8	0.97708	0.995978	0.994983	0.974624	0.977257
1.1	1.010395	1.001796	1.00249	1.012683	1.011355	1.1	1.01250	1.001791	1.002702	1.012688	1.011360
1.4	1.043659	1.007215	1.010001	1.05062	1.045365	1.4	1.04583	1.007383	1.010035	0.010505	1.045391
1.7	1.079002	1.012634	1.017512	1.088556	1.079303	1.7	1.07916	1.013259	1.017754	1.088701	1.079325
2.0	1.112266	1.017972	1.025023	1.126436	1.113166	2.0	1.11458	1.018443	1.025473	1.126650	1.113188

Config. c						Config. d					
Failure rate in p.u.	Q (p.u.)	F (p.u.)	ELC (p.u.)	EENS (p.u.)	EDLC (p.u.)	Failure rate in p.u.	Q (p.u.)	F (p.u.)	ELC (p.u.)	EENS (p.u.)	EDLC (p.u.)
0.5	0.826367	0.888262	0.871855	0.821634	0.826609	0.5	0.827362	0.887105	0.871061	0.821501	0.825632
0.8	0.929260	0.954663	0.948602	0.928736	0.930803	0.8	0.931596	0.955001	0.948220	0.928660	0.930420
1.1	1.032154	1.022301	1.025629	1.035591	1.034593	1.1	1.035831	1.022800	1.025844	1.035629	1.034707
1.4	1.138264	1.089611	1.103448	1.142282	1.137832	1.4	1.140065	1.090541	1.103932	1.142352	1.138599
1.7	1.237942	1.156959	1.181267	1.248726	1.240630	1.7	1.244300	1.158398	1.182021	1.248827	1.241862
2.0	1.340836	1.224404	1.260019	1.354924	1.343024	2.0	1.348534	1.226701	1.261039	1.355139	1.344757

Config. e					
Failure rate in p.u.	Q (p.u.)	F (p.u.)	ELC (p.u.)	EENS (p.u.)	EDLC (p.u.)
0.5	0.945289	0.949716	0.897101	0.892795	0.954016
0.8	0.975684	0.979232	0.958726	0.957103	0.981542
1.1	1.009119	1.010210	1.020663	1.021411	1.009282
1.4	1.042553	1.041884	1.083641	1.085719	1.037130
1.7	1.079027	1.072050	1.146619	1.150027	1.065084
2.0	1.112462	1.104212	1.210639	1.214335	1.093252

Config. f					
Failure rate in p.u.	Q (p.u.)	F (p.u.)	ELC (p.u.)	EENS (p.u.)	EDLC (p.u.)
0.5	0.901554	0.943850	0.895806	0.894422	0.944105
0.8	0.958549	0.978182	0.958059	0.957769	0.977584
1.1	1.020725	1.013369	1.020839	1.021116	1.011251
1.4	1.041451	1.048128	1.084674	1.084538	1.045059
1.7	1.139896	1.084225	1.149037	1.147885	1.079123
2.0	1.207254	1.120455	1.213928	1.211232	1.113316

**Table 18** The effect of changing the repair time of TRN on reliability indices of Configs. a-f.

Config. a					
Repair time in p.u.	Q (p.u.)	F (p.u.)	ELC (p.u.)	EENS (p.u.)	EDLC (p.u.)
0.5	0.941800	0.995147	0.992213	0.936583	0.943099
0.8	0.977133	0.998059	0.996956	0.974634	0.977275
1.1	1.010400	1.000971	1.001700	1.012685	1.011355
1.4	1.043660	1.003898	1.006048	1.050630	1.045365
1.7	1.079003	1.006745	1.010792	1.088560	1.079303
2.0	1.112270	1.009625	1.015535	1.126440	1.113170

Config. b					
Repair time in p.u.	Q (p.u.)	F (p.u.)	ELC (p.u.)	EENS (p.u.)	EDLC (p.u.)
0.5	0.943750	0.994832	0.991895	0.936563	0.943107
0.8	0.977084	0.997942	0.996912	0.974625	0.977257
1.1	1.012600	1.001037	1.001544	1.0127	1.01136
1.4	1.045833	1.004147	1.006561	1.050755	1.045391
1.7	1.079170	1.007211	1.011193	1.088702	1.079323
2.0	1.114585	1.010274	1.01621	1.1267	1.113192

Config. c					
Repair time in p.u.	Q (p.u.)	F (p.u.)	ELC (p.u.)	EENS (p.u.)	EDLC (p.u.)
0.5	0.909968	0.992966	0.989748	0.907776	0.910413
0.8	0.96463	0.997179	0.995806	0.963094	0.964236
1.1	1.016077	1.001391	1.001864	1.018412	1.017876
1.4	1.07074	1.005585	1.008388	1.073648	1.071406
1.7	1.122186	1.009779	1.014445	1.128802	1.124802
2	1.176849	1.013933	1.020503	1.183955	1.178099

Config. d					
Repair time in p.u.	Q (p.u.)	F (p.u.)	ELC (p.u.)	EENS (p.u.)	EDLC (p.u.)
0.5	0.912052	0.992445	0.989123	0.9076	0.909697
0.8	0.964169	0.996978	0.995631	0.963057	0.963969
1.1	1.019544	1.001492	1.002138	1.018433	1.018019
1.4	1.074919	1.006024	1.008646	1.07381	1.071996
1.7	1.127036	1.010519	1.014688	1.12911	1.125861
2	1.18241	1.015013	1.021196	1.18432	1.179579

Config. e					
Repair time in p.u.	Q (p.u.)	F (p.u.)	ELC (p.u.)	EENS (p.u.)	EDLC (p.u.)
0.5	0.96963	0.994199	0.989955	0.94458	0.976151
0.8	0.987843	0.99768	0.9962	0.97785	0.990432
1.1	1.00305	1.00116	1.001926	1.011086	1.004784
1.4	1.0213	1.004618	1.008172	1.0444	1.019136
1.7	1.039514	1.008052	1.013897	1.077596	1.033559
2	1.057754	1.011486	1.020143	1.111	1.048019

Config. f					
Repair time in p.u.	Q (p.u.)	F (p.u.)	ELC (p.u.)	EENS (p.u.)	EDLC (p.u.)
0.5	0.948187	0.994305	0.989712	0.945415	0.971127
0.8	0.979275	0.998529	0.996043	0.978138	0.988372
1.1	1.010363	1.002674	1.001846	1.010935	1.00584
1.4	1.041451	1.008021	1.008177	1.04373	1.02321
1.7	1.072539	1.011096	1.01398	1.07653	1.0408
2	1.103627	1.016043	1.020311	1.10933	1.05838

## 6 The Effect of Repair Time of TRN and DCB on the Reliability of Load Point

The impact of the repair time change of TRN and DCB on the reliability indices is investigated in this section and shown in Tables 18 and 19, respectively. For each grid, the amount of repair time is changed between 0.5 p.u and 2 p.u of the nominal repair time which is mentioned in the appendices, and the reliability indices have been evaluated. Then, the

amount of these indices has been divided by the nominal amount of the indices shown in Tables 4, 6, 8, 10, 12, and 14. Therefore, the per-unit amount of each index is obtained.

The most increase of EENS between 0.5 p.u and 2 p.u of the repair time of TRN is related to Config. d, which increases by 0.2768 p.u. The least increase of EENS between the failure rates of 0.5 p.u and 2 p.u is related to Config. f, which increases by 0.1639 p.u.

**Table 19** The effect of changing the repair time of DCB on reliability indices of Configs. a-f.

Config. a					
Repair time in p.u.	Q (p.u.)	F (p.u.)	ELC (p.u.)	EENS (p.u.)	EDLC (p.u.)
0.5	0.889814	0.990246	0.984306	0.877375	0.889828
0.8	0.956343	0.996134	0.993794	0.950974	0.956019
1.1	1.021040	1.001313	1.002886	1.024460	1.021948
1.4	1.087320	1.007781	1.012373	1.097830	1.087497
1.7	1.151805	1.012634	1.021465	1.171030	1.152903
2.0	1.216222	1.019104	1.030952	1.244100	1.217977

Config. b					
Repair time in p.u.	Q (p.u.)	F (p.u.)	ELC (p.u.)	EENS (p.u.)	EDLC (p.u.)
0.5	0.889586	0.989632	0.983793	0.877240	0.889826
0.8	0.956260	0.995978	0.993825	0.950963	0.956035
1.1	1.022920	1.002262	1.003088	1.024520	1.021887
1.4	1.087500	1.005404	1.012736	1.098020	1.087478
1.7	1.154170	1.013259	1.022385	1.171290	1.152950
2.0	1.218750	1.021113	1.032034	1.244442	1.217947

Config. c					
Repair time in p.u.	Q (p.u.)	F (p.u.)	ELC (p.u.)	EENS (p.u.)	EDLC (p.u.)
0.5	0.826400	0.985951	0.979497	0.821640	0.826646
0.8	0.929500	0.994396	0.992078	0.928750	0.930803
1.1	1.032160	1.002976	1.004194	1.035595	1.034593
1.4	1.138270	1.010706	1.016309	1.142285	1.137832
1.7	1.237945	1.018436	1.027959	1.248740	1.240703
2.0	1.340850	1.027712	1.040075	1.354930	1.342840

Config. d					
Repair time in p.u.	Q (p.u.)	F (p.u.)	ELC (p.u.)	EENS (p.u.)	EDLC (p.u.)
0.5	0.827366	0.984057	0.978897	0.821200	0.825041
0.8	0.931700	0.993743	0.991447	0.928600	0.930188
1.1	1.035833	1.003429	1.003997	1.035712	1.034855
1.4	1.140100	1.011177	1.017012	1.142600	1.138968
1.7	1.244500	1.020863	1.029562	1.249240	1.242712
2.0	1.348535	1.030548	1.042112	1.355715	1.345717

Config. e					
Repair time in p.u.	Q (p.u.)	F (p.u.)	ELC (p.u.)	EENS (p.u.)	EDLC (p.u.)
0.5	0.945290	0.988514	0.980066	0.892800	0.954016
0.8	0.975687	0.995475	0.992037	0.957105	0.981542
1.1	1.009120	1.002436	1.004008	1.021413	1.009282
1.4	1.042555	1.009398	1.015458	1.085720	1.037130
1.7	1.079030	1.016359	1.027429	1.150030	1.065084
2.0	1.112464	1.021000	1.038880	1.214340	1.093181

Config. f					
Repair time in p.u.	Q (p.u.)	F (p.u.)	ELC (p.u.)	EENS (p.u.)	EDLC (p.u.)
0.5	0.901560	0.987540	0.979689	0.894426	0.944105
0.8	0.958545	0.994652	0.991823	0.957800	0.977529
1.1	1.020725	1.002674	1.003957	1.021150	1.011251
1.4	1.077800	1.012299	1.016091	1.084550	1.045102
1.7	1.140000	1.021390	1.027697	1.147890	1.079123
2.0	1.207260	1.029412	1.039831	1.211234	1.113273

**7 The Effect of Simultaneous Change of the Failure Rate ( $\lambda$ ) and Repair Time ( $\mu$ ) of the Transformer on the EENS of Config. c**

Since a DC link between a generation point and the load point has a significant impact on the improvement of the load point reliability indices of a four-terminal grid and minimizing the amount of energy not supplied, the effect of simultaneous change of the failure rate ( $\lambda$ ) and repair time ( $\mu$ ) of the transformer on the EENS of Config. c is investigated by multivariate linear regression. This study aims to estimate EENS when the failure rate and repair time change with identical steps of 0.1, from 0.5 p.u. to 2 p.u. of their nominal value. The multivariate linear regression is carried out in Jupyter Notebook using a gradient descent algorithm to minimize the cost function. The result is shown in Fig. 5.

In this study, the hypothesis function is defined as:

$$h_{\theta}(x_i) = \theta_0 + \theta_1 x_1 + \theta_2 x_2 \tag{1}$$

where  $x_i$  is the input of the  $i$ th training example and  $\theta_i$  is the parameter of the model and it should be calculated. And the cost function is:

$$J(\theta_0, \theta_1, \theta_2) = \frac{1}{2m} \sum_{i=1}^m (h_{\theta}(x_i) - y_i)^2 \tag{2}$$

Where  $y_i$  is the actual output.

And the equation for calculating  $\theta_j$  in the gradient descent process for multiple variables would be:

$$\theta_j := \theta_j - \alpha \frac{1}{m} \sum_{i=1}^m (h_{\theta}(x^{(i)}) - y^{(i)}) x_j^{(i)} \tag{3}$$

for  $j = 0, 1, 2, \dots, n$

Where  $x_j^{(i)}$  is the value of feature  $j$  in the  $i$ th training example,  $x^{(i)}$  is the input (feature) of the  $i$ th training example,  $m$  is the number of training examples, and  $n$  is the number of features.

The convergence of the cost function is checked after 400 iterations, and  $\theta_0$ ,  $\theta_1$ , and  $\theta_2$  are calculated. Based on this calculation, we have  $\theta_0 = 136471.72892594$ ,  $\theta_1 = 13291.19042663$ ,  $\theta_2 = 13291.19042663$ .

Based on the findings from multivariate linear regression, we can show results in Table 20.

### 8 Conclusion

In this paper, six configurations of MTDC grids are introduced and studied. These grids include four four-terminal grids with different numbers of DC links, two four-terminal grids with the same number of DC links, and a tap station in two different grid locations. The numerical analyses of the obtained results show that a DC link between a generation point and the load point significantly impacts the improvement of a four-terminal grid's load point reliability indices and minimizes the amount of energy not supplied. However, a DC link between two generation points slightly influences the improvement of the load point reliability indices. The existence of both links (one between a generation point and the load point and one between two generation points) improves the load point indices slightly in comparison with the state in which there is a link between a generation point and the load point. However, considering the cost-benefit issues, this slight improvement may not be worth it

against the cost of implementing a new DC transmission line. Adding a tapping station to the grid considerably impacts the grid's reliability, but this improvement depends on the generation capacity and the location of the tapping station. Thus, it is necessary to consider the cost of each configuration and the location of the new generation points or DC links alongside the reliability of the corresponding configuration for different transmission systems to have a reliable and affordable energy transmission system.

### 9 Acknowledgments

The authors acknowledge the funding support of the Babol Noshirvani University of Technology through grant program No. BNUT/964112034/97.

### Intellectual Property

The authors confirm that they have given due consideration to the protection of intellectual property associated with this work and that there are no impediments to publication, including the timing to publication, with respect to intellectual property.

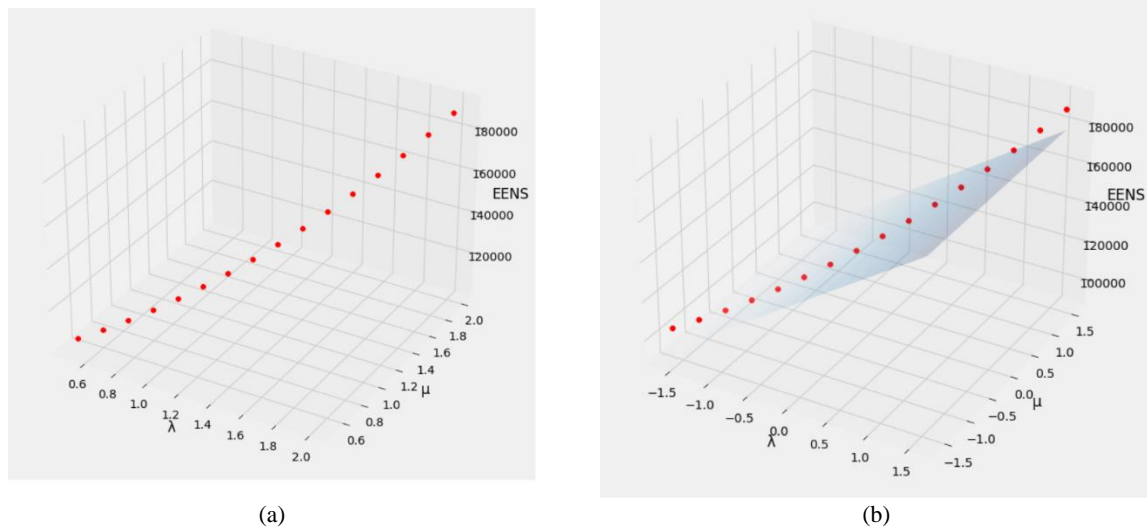


**Fig. 5** Considering the effect of simultaneous change of the transformer's failure rate ( $\lambda$ ) and repair time ( $\mu$ ) on the EENS of Config. c using multivariate linear regression. (a): Plot configurations. (b): After feature normalization.

**Table 20** The effect of simultaneous change of the failure rate ( $\lambda$ ) and repair time ( $\mu$ ) of the transformer between 0.5 and 2 of the nominal values on the EENS of Config. c.

$\lambda$ (p.u)	0.5	0.6	0.7	0.8	0.9	1	1.1	1.2
$\mu$ (p.u)	0.5	0.6	0.7	0.8	0.9	1	1.1	1.2
EENS (MWh/yr)	104830	107310	110230	113590	117410	121670	126370	131520
$\lambda$ (p.u)	1.3	1.4	1.5	1.6	1.7	1.8	1.9	2
$\mu$ (p.u)	1.3	1.4	1.5	1.6	1.7	1.8	1.9	2
EENS (MWh/yr)	137120	143150	149630	156540	163900	171690	179920	188580

## Funding

No funding was received for this work.

## Credit Authorship Contribution Statement

**S. P. Ramezanzadeh:** Formal analysis, Conceptualization, Methodology, Software, Investigation, Writing - Original Draft, Writing - Review & Editing, Resources, Visualization, Validation. **M. Mirzaie:** Data Curation, Supervision, Visualization, Conceptualization, Project administration, Resources, Validation. **M. Shahabi:** Data Curation, Visualization, Investigation, Validation, Software, adviser, Writing - Review & Editing.

## Declaration of Competing Interest

The authors hereby confirm that the submitted manuscript is an original work and has not been published so far, is not under consideration for publication by any other journal and will not be submitted to any other journal until the decision will be made by this journal. All authors have approved the manuscript and agree with its submission to "Iranian Journal of Electrical and Electronic Engineering".

## References

- [1] P. Hartel, T. Varna, T., et al. "Review of investment model cost parameters for VSC HVDC transmission infrastructure", *Electric Power System Research*, Vol. 151, pp. 419-431, 2017.
- [2] T. Varna, P. Hartel, "Estimation of investment model cost parameters for VSC HVDC transmission infrastructure", *Electric Power System Research*, Vol. 160, pp. 99-108, 2018.
- [3] W. Zibo, "HVDC Transmission System Reliability Evaluation Based on Condition-dependent Failure Models of Converters and Transformers", *Theses and Dissertations*, 2017.
- [4] Z. Xu, H. Liu, et al. "Power supply capability evaluation of distribution systems with distributed generations under differentiated reliability constraint", *International Journal of Electrical Power & Energy Systems*, Vol. 134, 2022, 107344.
- [5] C. MacIver, K. R. W. Bell, D. P. Nedic, "A Reliability Evaluation of Offshore HVDC Grid Configuration Options", *IEEE Transactions on Power Delivery*, Vol. 31, No.2, pp. 810-819, 2016.
- [6] T. F. Agajie, et al. "Reliability enhancement and voltage profile improvement of distribution network using optimal capacity allocation and placement of distributed energy resources", *Computers & Electrical Engineering*, Vol. 93, 2021, 107295.
- [7] L. Shen, Q. Tang, Y. Wang, F. Song "A Review on VSC-HVDC Reliability Modeling and Evaluation Techniques", *Asia Conference on Power and Electrical Engineering*, 2017.
- [8] W. Feng, L. A. Tuan, et al. "A New Approach for Benefit Evaluation of Multi-terminal VSC-HVDC Using A Proposed Mixed AC/DC Optimal Power Flow", *IEEE Transactions on Power Delivery*, Vol. 29, No. 1, pp. 432-443, 2014.
- [9] S. Zadhast, M. Fotuhi-Firuzabad, F. Aminifar, R. Billinton, et al. "Reliability Evaluation of an HVDC Transmission System Tapped by a VSC Station", *IEEE Transactions on Power Delivery*, Vol. 25, No. 3, pp. 1962-1970, 2010.
- [10] A. Khanjanzadeh, et al. "Integrated multi-area power system with HVDC tie-line to enhance load frequency control and automatic generation control", *Electrical Engineering*, Vol. 102, No.3, pp. 1223-1239, 2020.
- [11] M. Elgeziry, et al. "Enhancing wind power transfer and protection of actual Egyptian 220 kV HVAC transmission system with multi-terminal VSC-HVDC system", *Electrical Engineering*, Vol. 103, pp. 1837-1847, 2021.
- [12] J. Martinez-Velasco, J. Magnusson, "Parametric analysis of the hybrid HVDC circuit breaker", *International Journal of Electrical Power & Energy Systems*, Vol. 84, pp. 284-295, 2017.
- [13] Y. Guo, H. Gao, Q. Wu "A combined reliability model of VSC-HVDC connected offshore wind farms considering wind speed correlation", *IEEE Transactions on Sustainable Energy*, Vol. 8, No. 4, pp. 1637-1646, 2015.
- [14] B. Hu, K. Xie, H. Tai, "Reliability Evaluation and Weak Component Identification of A  $\pm 500$  kV HVDC Transmission Systems With Double-Circuit Lines on the Same Tower", *IEEE Transactions on Power Delivery*, Vol. 33, No. 4, pp. 1716-1726, 2018.

- [15] B. Hu, K. Xie, H. Tai, "Optimal reliability allocation of A  $\pm 800$  kV ultra HVDC transmission systems", *IEEE Transactions on Power Delivery*, Vol. 33, No. 3, pp. 1174-1184, 2017.
- [16] J. Contreras-Jimenez, F. Rivas-Dávalos, "Multi-state system reliability analysis of HVDC transmission systems using matrix-based system reliability method", *International Journal of Electrical Power & Energy Systems*, Vol. 100, pp. 265-278, 2018.
- [17] Y. Hua, S. Li, Z. Wu, "Short-Term Reliability Assessment of UHVdc Systems Based on State Aggregation With SMP", *IEEE Transactions on Reliability*, Vol. 68, No. 3, pp. 790-799, 2019.
- [18] B. Tuinema, R. Getreuer, et al. "Reliability analysis of offshore grids-An overview of recent research", *Wiley Interdisciplinary Reviews: Energy and Environment*, Vol. 8, No. 1, pp. e309, 2019.
- [19] S. P. Ramezanzadeh, M. Mirzaie, M. Shahabi, "Reliability assessment of different HVDC transmission system configurations considering transmission lines capacity restrictions and the effect of load level", *International Journal of Electrical Power & Energy Systems*, Vol. 128, 2021, 106754.



S. P. Ramezanzadeh received the B.Sc. and M.Sc. degrees from Babol Noshirvani University of Technology, Babol, Iran, in 2017 and 2020, respectively, all in electrical engineering. He has been a Ph.D. candidate at Tarbiat Modares University, Tehran, Iran, since 2021. His research interests include high-voltage engineering and also power system transients and reliability assessment of power system equipment.



M. Mirzaie received a B.Sc. degree from Shahid Chamran University, Ahvaz, Iran, in 1997, and the M.Sc. and Ph.D. degrees from the Iran University of Science and Technology, Tehran, Iran, in 2000 and 2007, respectively, all in electrical engineering. He has been a Professor at the Babol Noshirvani University of Technology, Babol, Iran, since 2020. He is the author of more than 120 journal and conference papers.

His research interests include high-voltage engineering and also operation problems and condition assessment/monitoring of high-voltage equipment.



M. Shahabi (S'00-M'10) received a B.Sc. degree in electrical engineering from Tabriz University, Tabriz, Iran, in 1998, and the M.Sc. and Ph.D. degrees in electric power engineering from Tarbiat Modares University, Tehran, Iran, in 2001 and 2009, respectively. Since 2010, he has been with the Babol Noshirvani University of Technology, Babol, Iran, where he is currently an Associate Professor.

His current research interests include microgrids, power system operation, and control in the presence of embedded generation resources.



© 2023 by the authors. Licensee IUST, Tehran, Iran. This article is an open-access article distributed under the terms and conditions of the Creative Commons Attribution-NonCommercial 4.0 International (CC BY-NC 4.0) license (<https://creativecommons.org/licenses/by-nc/4.0/>).